Elastic properties of $B2$-NiTi and $B2$-PdTi

G. Bihlmayer, R. Eibler, and A. Neckel
Institute of Physical Chemistry, University of Vienna, Währingerstraße 42, A-1090 Vienna, Austria
(Received 8 March 1994; revised manuscript received 11 July 1994)

Elastic constants of the high-temperature phases of the shape-memory alloys NiTi and PdTi are determined by means of full-potential linearized augmented-plane-wave total-energy calculations. Thereby, insight into the driving mechanism of the martensitic transformation of these alloys can be obtained. In the case of NiTi, the c' and c_{44} moduli are found to be low and to decrease with rising pressure. We find that the (parent) PdTi phase is metastable with respect to tetragonal deformations. From these data, we can explain the different transformation behavior of the two alloys. In the case of PdTi, the Ti-Ti bonding seems to be responsible for the formation of the martensitic phases. Experimental data, if available, are found to be in good agreement with the results of our calculations.

I. INTRODUCTION

In the last few decades shape-memory metals have found widespread applications in the fields of engineering and medicine. Despite of their technological importance, the driving forces of their behavior on the atomic level are still not well understood. Since its discovery,[1] the shape-memory effect (SME) of NiTi has been a focus of investigations in this field,[2,3] possibly due to the simplicity of the structures involved in the transformation ($B2$ or CsCl structure in the high and $B19'$ or AuCd structure in the low-temperature phase) and the convenient transformation temperature of 333 K. In two preceding papers[4,5] we have performed a comparative study of NiTi and another SME alloy, PdTi, in order to find an explanation for the profound differences in the transformation mechanism and temperature (790 K for PdTi) of these alloys despite their similarity in structure. In these papers we discussed the electronic structure of the parent and martensitic phases. Specifically, we found nesting features in the Fermi surface of $B2$-NiTi causing anomalies in the phonon spectra[6] that are believed to cause an incommensurate-to-commensurate phase transition from the $B2$ to the "premartensitic" R phase of NiTi. In contrast, no such premartensitic phase has been found in the PdTi system and our calculation showed that nesting is largely reduced due to the formation of "bottlenecks" in the Fermi surface of $B2$-PdTi. Some recent results[7] seem to confirm these findings. This paper, however, is concerned with the energetic aspects of the transformation.

Several mechanisms for the martensitic transformation of β-phase alloys have been proposed,[8,9] some of them including the influence of defects.[10,11] In all cases, there are two major factors determining the transformational behavior of the phases: (i) the presence of anomalies in the phonon system, especially near the transformation temperature and (ii) the temperature dependence of the elastic constants. Unfortunately, our calculations cannot simulate temperature effects in an easy way. Nevertheless, the knowledge of the limiting values of the elastic constants for vanishing temperature and their volume dependence can provide useful information about the behavior of these properties near the transformation temperature. Since the volume dependence of the elastic constants should reflect at least one part of their temperature dependence, we think that it is instructive to study this influence.

Since first-principles total-energy calculations are quite sensitive to computational details, we will describe the employed method thoroughly in the following section. The results will be presented in Sec. III and a discussion of the phase transformation will be given in Sec. IV.

II. COMPUTATIONAL ASPECTS

A. Total energies

For the calculation of the total energies E of the phases we used the full-potential linearized augmented-plane-wave (FLAPW) method,[12] for it is known to be precise in a wide range of materials and structures. The Barth-Hedin exchange correlation potential[13] was used, and scalar-relativistic corrections for the valence electrons were included. The core states (Ni and Ti: [Ar]; Pd: [Kr]) were treated in a fully relativistic fashion. In a spin-polarized test calculation no evidence for magnetic moments in NiTi was found. Therefore, spin polarization was not included in our further calculations.

Each point of the energy surface was calculated to self-consistency with a remaining pressure of maximum 250 mbar or approximately 2 μRy total-energy difference between the last two iterations. The multipole expansion of the potential and charge density in the muffin-tin spheres was cut off at $l=8$. In the interstitial region, plane waves with reciprocal lattice vectors up to $|\mathbf{G}|=10$ were included. The plane-wave basis was tested for convergence and, typically, 200 basis functions per atom were found to yield sufficient accuracy in all cases. The $\mathbf{k}$-point sampling in the Brillouin zone (BZ) was also tested for convergence, and we found a regular mesh of 4096 points in the BZ to give accurate results. This corresponds to 165, 405, and 525 $\mathbf{k}$ points in the irreducible part of the BZ for cubic, tetragonal, and trigonal structures, respectively. The BZ integration was performed by means of the linearized tetrahedron method.[14]

The muffin-tin radii were kept constant for all calcula-

tions and chosen to be 2.300 a.u. for Ni and 2.150 a.u. for Ti in NiTi and 2.537 a.u. for Pd and 2.416 a.u. for Ti in PdTi, respectively. A mesh of 331 points with a logarithmic step size of 0.029 was used for the radial functions.

B. Elastic constants

For the calculation of the elastic constants we applied the following procedure: We started with the experimental geometries and varied the volume of the phases in order to determine the bulk modulus B and the equilibrium volume V_0 at $T=0$ K. We calculated total energies for seven different volumes and used a second-order Birch fit,[15] that is

$$E(V)=E_0+\tfrac{9}{8}B_0V_0\left[\left[\frac{V_0}{V}\right]^{2/3}-1\right]^2, \tag{1}$$

where E_0, B_0, and V_0 denote the equilibrium energy, bulk modulus, and volume, respectively. Fitting errors were less than 10^{-5} Ry. The tetragonal and trigonal deformations for the calculation of the shear moduli c' and c_{44} were applied to the cubic structure with the equilibrium volume.

The deformation tensor for the tetragonal distortion can be written as

$$\overleftrightarrow{\epsilon}_{\text{tet}}=\begin{pmatrix}-\frac{\delta}{2} & 0 & 0\\ 0 & -\frac{\delta}{2} & 0\\ 0 & 0 & +\delta\end{pmatrix}, \tag{2}$$

conserving the volume of the phase up to second order in the deformation parameter δ. This parameter was varied in a range from -0.067 to $+0.067$ resulting in c/a ratios from 0.9 to 1.1. We calculated the energy density $U=E/V$ of seven to nine deformed phases and fitted a polynomial of fourth order to the results. Again, this yielded fitting errors less than 10^{-5} Ry. With the relations

$$B_0=V_0\left[\frac{\partial^2E}{\partial V^2}\right]_{V_0}=\frac{1}{3}(c_{11}+2c_{12})$$

and (3)

$$c'=\frac{1}{3}\left[\frac{\partial^2U}{\partial\delta^2}\right]_{\delta=0}=\frac{1}{2}(c_{11}-c_{12})$$

two of the principal moduli of the phase can be calculated.

The c_{44} modulus can be calculated directly from trigonal or monoclinic distortions with deformation tensors

$$\overleftrightarrow{\epsilon}_{\text{tri}}=\begin{pmatrix}\delta^2 & \delta & \delta\\ \delta & \delta^2 & \delta\\ \delta & \delta & \delta^2\end{pmatrix} \text{ or } \overleftrightarrow{\epsilon}_{\text{m}}=\begin{pmatrix}0 & \frac{\delta}{2} & 0\\ \frac{\delta}{2} & 0 & 0\\ 0 & 0 & \frac{\delta^2}{4-\delta^2}\end{pmatrix}. \tag{4}$$

The trigonal tensor changes the volume to the third order in the deformation parameter, thus being slightly inferior to the monoclinic deformation that is often applied. Nevertheless, because of the relation

$$c_{44}=\tfrac{1}{12}\left[\frac{\partial^2U}{\partial\delta_{\text{tri}}^2}\right]_{\delta=0}=\frac{1}{4}\left[\frac{\partial^2U}{\partial\delta_{\text{m}}^2}\right]_{\delta=0}, \tag{5}$$

the deformation parameter can be chosen much smaller in this case. The convenience of the higher symmetry of the trigonal phase makes this method preferable. As before, a polynomial of fourth order was fitted to seven points of the energy-surface, with fitting errors less than 10^{-4} Ry.

III. RESULTS

In Table I we present the experimental[16] and calculated elastic constants of $B2$-NiTi and the relative errors. The experiments were conducted near room temperature and the temperature dependence of the elastic constants was determined in a narrow range around this value. From these experiments, it can be seen that, whereas B and c' remain approximately constant, c_{44} shows pronounced softening with decreasing temperature.

The bulk-modulus is given at the experimental volume and is—apart from the typical overbinding that is often attributed to the local density approximation—in quite good agreement with experiment. The equilibrium lattice constant is 1% lower than the experimental one.

The c' modulus of NiTi is known to be small, and our calculations yield a still smaller value for c'. From Fig. 1 we can see that the minimum of the U_{tet} vs c/a curve is not at the expected value $c/a=1.0$. The lowest curve was calculated for the equilibrium volume V_0, the upper one for the experimental, and the in-between curve for an intermediate volume. We note that the energy differences resulting from these deformations are very small (i.e., less than 1 mRy over the range of deformation), so care has to be taken to use well-converged results.

The calculated value of c_{44} is 34% higher than the experimental one. Our calculations are valid at absolute zero only and the experimental value was taken in a small interval at room temperature, therefore better agreement of our theoretical value with an experimental value near absolute zero can be expected.

We find that the calculated c' modulus *softens* with rising pressure, but the effect is rather small. Recent experi-

TABLE I. Elastic constants and bulk moduli of $B2$-NiTi and $B2$-PdTi. Calculated values refer to 0 K, while experimental data were measured at room temperature. Experimental values taken from Ref. 16.

	NiTi (expt.) (GPa)	NiTi (calc.) (GPa)	Error (%)	PdTi (calc.) (GPa)
c_{11}	162.4	178.2	+9.3	109.3
c_{12}	129.2	147.6	+13.3	160.9
c_{44}	34.8	49.0	+34.1	0.6
c'	16.6	15.3	−8.2	−25.8
B	140.3	157.8	+11.7	143.7

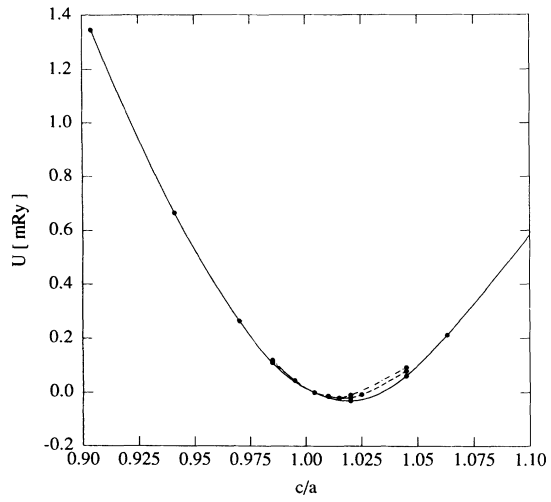

FIG. 1. Strain energy density U of $B2$-NiTi at the experimental (dot-dashed), equilibrium (full) and an intermediate volume (dashed line) as a function of the c/a ratio.

mental data[17] of $Ni_{48}Ti_{50}Fe_2$ confirm these results. In contrast, c_{44} is experimentally found to harden with rising pressure. The authors of this reference agreed, however, that the applied pressure (0.6 GPa) was probably too small to give the correct behavior at the phase transition (6 GPa). Figure 2 shows the theoretical variation of the c' and c_{44} moduli with the volume of the unit cell.

In the case of PdTi, the situation is not so simple. As to the bulk modulus, we find PdTi to be approximately 10% softer than NiTi, this result being quite reasonable. The lattice constant is 1.5% smaller at equilibrium geometry ($T=0$ K) compared with the experimental value at $T=790$ K.

The c' modulus turns out to be negative, thus indicating an instability of cubic PdTi with respect to tetragonal distortions. Since $B2$-PdTi is, in fact, unstable at 0 K, we can understand this instability, but we want to investigate this point further. As can be seen from Fig. 3, the U_{tet} vs c/a curve has two minima at $c/a=1.37$ and 0.85. It is interesting that the nearest neighbor Ti-Ti (and also Pd-Pd) distances are equal and ≈ 5.3 a.u. in both geometries. Furthermore, we notice that the nearest-neighbor Ti-Ti distance in the low-temperature phase $B19$-PdTi is also 5.3 a.u. If we assume that the stabilization of the two described geometries is due to Ti-Ti bonding, we can also explain why the minimum at $c/a=1.37$ is deeper than its counterpart at $c/a=0.85$. In the first case, eight nearest-neighbor Ti-Ti bonds can be formed on the top and bottom squares of the tetragonal unit cell, in the second case only four Ti-Ti distances on the sides of the unit cell are suited for efficient bonding. To illustrate this effect, Fig. 4 shows the valence-electron density in the Ti-Ti directions (parallel to the crystallographic c and a axis). First, we notice that the electron density is lowered as the cuts move further away from the large Pd atom. On the left, a small maximum in the valence-electron density appears with increasing c/a ratio in the bonding direction parallel to the crystal's c axis. It is most pronounced at a Ti-Ti distance of 5.3 a.u. corresponding to a c/a ratio of 1.37. The same holds true for the direction parallel to the a axis of the crystal as the c/a ratio is lowered (right side of Fig. 4). These findings suggest that, indeed, tetragonal deformations enable the formation of weak Ti-Ti bonds, thus destabilizing the cubic geometry of $B2$-PdTi.

The same ideas can be applied to NiTi, and we would expect two minima at $c/a=1.09$ and 0.95. In fact, no such minima can be found, and we notice that there is only one minimum at the average c/a value of 1.02.

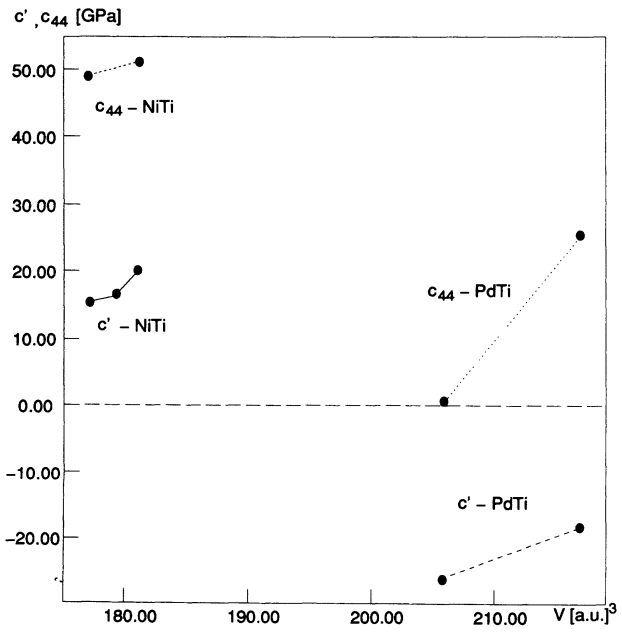

FIG. 2. Volume dependence of the elastic constants c_{44} and c' of $B2$-NiTi and $B2$-PdTi.

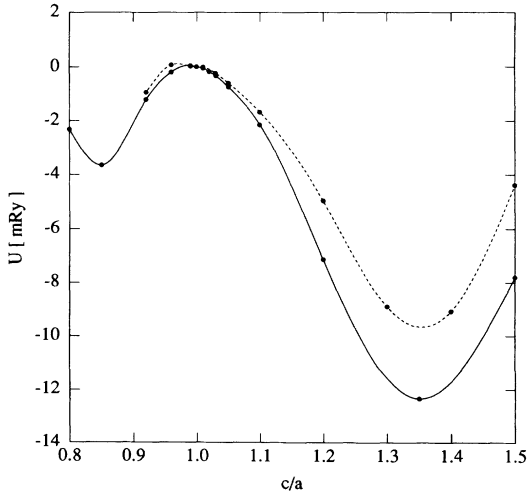

FIG. 3. Strain-energy density U of $B2$-PdTi at the experimental (dashed) and equilibrium (full line) volume as a function of the c/a ratio.

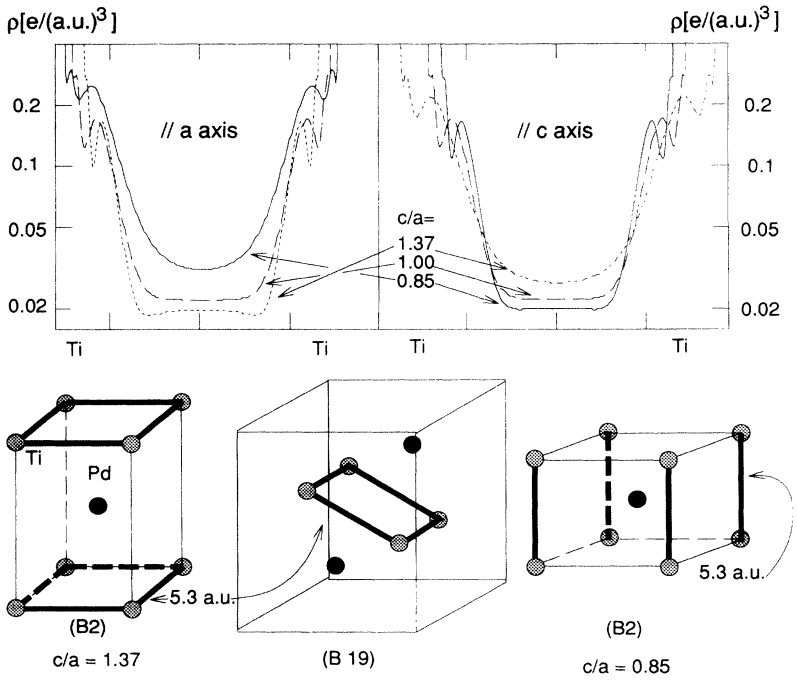

FIG. 4. Top: valence-electron density ρ along the Ti-Ti directions parallel to the a (left) and c axis (right) of tetragonally deformed $B2$-PdTi for various c/a ratios. Bottom: Geometries of the tetragonally deformed $B2$-PdTi structure at c/a ratios corresponding to the minima of Fig. 3 and of $B19$-PdTi. Thick lines indicate where the Ti-Ti distance is at its optimal value of 5.3 a.u.

Figure 3 also shows the variation of the strain-energy density of $B2$-PdTi with respect to tetragonal deformations at two different volumes. We see that, as the pressure decreases, the c' modulus becomes less negative (Fig. 2), and the minima are not so pronounced.

The deeper minimum is very close to $c/a=\sqrt{2}$, corresponding to the $L1_0$ structure. We also calculated NiTi in the $L1_0$ structure, but no stabilization of this geometry was found.

IV. DISCUSSION

In order to study the influence of the elastic constants on the transformation behavior of NiTi, we follow the procedure adopted by Pushin, Kondrat'ev, and Khachin.[3] These authors derived conditions for the formation of an intermediate shear structure (ISS) that acts as a precursor for the R phase of NiTi. Three waves in the [112] and [110] directions are involved in the transition, and an expansion of the free energy of the anharmonic crystal in these lattice-displacement waves was carried out. Finally, the authors arrive at conditions, expressed in terms of elastic constants, which determine whether an ISS, ω or $9R$ structure is formed from the parent phase. These structures appear also at martensitic transitions of other bcc-type alloys. If the anisotropy parameter $A=c_{44}/c'$ gets too large by softening of c', a shear in the $[110]\langle 1\bar{1}0\rangle$ direction easily leads to the formation of the $9R$ phase or directly to the AuCd structure. Otherwise, if c_{44} (and A) is drastically lowered, ω-phase formation is favored. In the case of NiTi, both elastic moduli are decreasing, so the anisotropy constant remains small (experiment 2.1, calculation 3.2) and the complex three-wave reconstruction, leading to an ISS formation, of the phase occurs.

In the case of PdTi, the situation is much different. At temperatures well above the martensitic transformation temperature M_s both shear moduli are positive; at absolute zero only c_{44} has a small but non-negative value. Therefore, c' should go to zero at M_s, while c_{44} should still be positive. Thus, A gets very large and the direct $B2\rightarrow B19$ transformation occurs. As c' gets very small due to the destabilizing effect of the Ti-Ti bonding, the (110) planes are free to move in the $[1\bar{1}0]$ direction to form the AuCd structure. A direct transformation path from $B2$- to $B19$-PdTi involves a deformation with the strain tensor ($\epsilon_{xx}=\epsilon_{xy}=\epsilon_{yy}=\delta/2$, $\epsilon_{zz}=-\delta$, $\epsilon_{yz}=\epsilon_{zx}=0$) with $\delta=0.1$ and a lattice-displacement wave $\mathbf{u}(\mathbf{r})=a_0\mathbf{e}\sin(\mathbf{q}\cdot\mathbf{r})$ with $\mathbf{q}$ in the [110] direction and $\mathbf{e}=0.09\langle 1\bar{1}0\rangle$. The energy change associated with the orthorhombic deformation is $U=(\delta^2/2)(3c'-c_{44})$ and the dispersion relation (in the long-wavelength limit) of a wave in the [110] direction with the indicated polarization depends solely on the c' modulus. Since c' vanishes as the transformation temperature is reached (while all other elastic constants remain finite), this direct transformation path could in fact lead to the geometry of the martensitic phase. So far, no formation of an intermediate phase has been observed in the transformation of PdTi. In fact, studies of $Ni_{1-x}Pd_xTi$ alloys[18] have shown that the mechanism changes from a typical $B2\rightarrow R\rightarrow B19'$ sequence at $x=0$ gradually, via mixed types, to the direct $B2\rightarrow B19$ mechanism at $x=1$. Together with the mechanism, the shape-memory parameters (e.g., maximum reversible deformation) change with stoichiometry.

From the differences in the calculated elastic constants we can explain the different transformation behavior of the NiTi and PdTi alloys. Experimental investigations of the temperature dependence of the elastic constants of $B2$-PdTi would be helpful to verify this model.

ACKNOWLEDGMENTS

We gratefully acknowledge the financial support of the Austrian Fonds zur Förderung der Wissenschaftlichen Forschung (Project No. P-9183-PHY) and the valuable support and grant of computer time of the Vienna University Computer Center. Furthermore, we would like to thank R. Podloucky for helpful discussions.

[1]F. E. Wang, W. J. Buehler, and S. J. Pickart, J. Appl. Phys. **36**, 3232 (1965).
[2]S. A. Shabalovskaya, Phys. Status Solidi B **132**, 327 (1985).
[3]V. G. Pushin, V. V. Kondrat'ev, and V. N. Khachin, Sov. Phys. J. **28**, 341 (1985).
[4]G. Bihlmayer, R. Eibler, and A. Neckel, Ber. Bunsenges. Phys. Chem. **96**, 1626 (1992).
[5]G. Bihlmayer, R. Eibler, and A. Neckel, J. Phys.: Condens. Matter **5**, 5083 (1993).
[6]H. Tietze, M. Müllner, and B. Renker, J. Phys. C **17**, L529 (1984).
[7]G. L. Zhao and B. N. Harmon, Phys. Rev. B **48**, 2031 (1993).
[8]M. J. Kelly and W. M. Stobbs, Phys. Rev. Lett. **45**, 992 (1980).
[9]E. V. Savushkin, V. B. Lapin, and V. E. Egorushkin, J. Phys.: Condens. Matter **3**, 9185 (1991).
[10]D. A. Vul and B. N. Harmon, Phys. Rev. B **48**, 6880 (1993).
[11]V. V. Kulagina and M. F. Zhorovkov, Solid State Phys. **1**, 1 (1992).
[12]E. Wimmer, H. Krakauer, M. Weinert, and A. J. Freeman, Phys. Rev. B **24**, 864 (1981).
[13]U. v. Barth and L. Hedin, J. Phys. C **5**, 1629 (1972).
[14]O. Jepsen and O. K. Andersen, Solid State Commun. **9**, 1763 (1971); G. Lehmann and M. Taut, Phys. Status Solidi **54**, 469 (1972).
[15]F. Birch, J. Geophys. Res. **83**(B3), 1257 (1978).
[16]O. Mercier, K. N. Melton, G. Gremaud, and J. J. Hägi, J. Appl. Phys. **51**, 1833 (1980).
[17]A. I. Lotkov, V. A. Goncharova, V. P. Lapshin, V. N. Grishkov, and M. N. Podlevskikh, Dokl. Akad. Nauk SSSR **330**, 191 (1993).
[18]V. P. Sivoka, A. S. Savvinov, V. P. Voronin, and V. N. Khachin, Phys. Met. Metallogr. (USSR) **56**, 112 (1983).

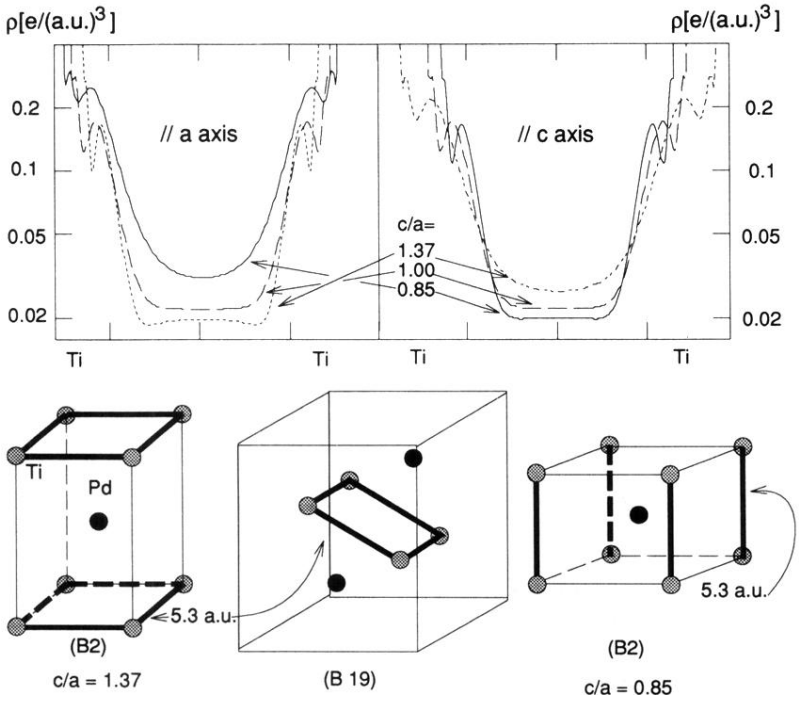

FIG. 4. Top: valence-electron density ρ along the Ti-Ti directions parallel to the a (left) and c axis (right) of tetragonally deformed $B2$-PdTi for various c/a ratios. Bottom: Geometries of the tetragonally deformed $B2$-PdTi structure at c/a ratios corresponding to the minima of Fig. 3 and of $B19$-PdTi. Thick lines indicate where the Ti-Ti distance is at its optimal value of 5.3 a.u.